^{1}H NMR based Metabolic Signatures in Liver and Brain in Rat Model of Hepatic Encephalopathy.

Anjana Pathania[1], Atul Rawat[2,4], Sitender Singh Dahiya[1], Saurabh Dhanda[3], Ravi Pratap Barnwal[5], Bikash Baishya[4], Rajat Sandhir[1]*

[1]Department of Biochemistry, Basic Medical Science Block-II, Panjab University, Chandigarh, 160014, India.
[2]Department of Surgery, IU Health Comprehensive Wound Centre, Indiana Center for Regenerative Medicine and Engineering, Indiana University School of Medicine, Indianapolis, IN, 46202, USA.
[3]Department of Biochemistry, Dr. Rajendra Prasad Government Medical College, Kangra at Tanda, Himachal Pradesh, India.
[4]Centre for Biomedical Magnetic Resonance (CBMR), SGPGIMS Campus, Lucknow, Uttar Pradesh, India.
[5]Department of Biophysics, Panjab University, Chandigarh, India.

***Corresponding author:**
Prof. Rajat Sandhir, Ph.D.,
Department of Biochemistry,
Basic Medical Sciences Block-II
Sector-25, Panjab University,
Chandigarh 160014, India.
Tel: 91-172-25344131;
Fax: 91-172-2541022
Email: sandhir@pu.ac.in

Abbreviations: Alkaline phosphatase (ALP); Bile duct ligation (BDL); Branched chain amino acids (BCAAs); Hepatic Encephalopathy (HE); Human Metabolome Database (HMDB); Nuclear Magnetic Resonance (NMR); Principal component analysis (PCA); Partial least squares discrimination analysis (PLS-DA); Tricarboxylic acid (TCA); Variable influence on projection (VIP).

This is the author's manuscript of the article published in final edited form as:

Pathania, A., Rawat, A., Dahiya, S. S., Dhanda, S., Barnwal, R. P., Baishya, B., & Sandhir, R. (2020). 1H NMR based Metabolic Signatures in Liver and Brain in Rat Model of Hepatic Encephalopathy. Journal of Proteome Research. https://doi.org/10.1021/acs.jproteome.0c00165

Abstract

Hepatic Encephalopathy (HE) is a debilitating neuropsychiatric complication associated with acute and chronic liver failure. It is characterized by diverse symptoms with variable severity that includes cognitive and motor deficits. The aim of the study is to assess metabolic alterations in brain and liver using nuclear magnetic resonance (NMR) spectroscopy and subsequent multivariate analyses to characterize metabolic signatures associated with HE. HE was developed by bile duct ligation (BDL) that resulted in hepatic dysfunctions and cirrhosis as shown by liver function tests. Metabolic profiles from control and BDL rats indicated increased levels of lactate, branched chain amino acids (BCAAs), glutamate and choline in liver, whereas levels of glucose, phenylalanine and pyridoxine were decreased. In case of brain, the levels of lactate, acetate, succinate, citrate and malate were increased, while glucose, creatine, isoleucine, leucine and proline levels were decreased. Furthermore, neurotransmitters such as glutamate and GABA were increased, whereas choline and myo-inositol were decreased. The alterations in neurotransmitter levels resulted in cognitive and motor defects in BDL rats. A significant correlation was found between alterations in NAA/choline, choline/creatine and NAA/creatine with behavioural deficits. Thus, the data suggests impairment in metabolic pathways such as tricarboxylic acid (TCA) cycle, glycolysis and ketogenesis in liver and brain of animals with HE. The study highlights that metabolic signatures could be potential marker to monitor HE progression and to assess therapeutic interventions.

Keywords: Behaviour; Brain; Energy metabolism; Hepatic encephalopathy; Metabolomics; Liver, Nuclear Magnetic Resonance Spectroscopy.

Introduction

Hepatic encephalopathy (HE) is defined as "brain dysfunction resulting from liver insufficiency and/or portal systemic shunting that exhibits a wide spectrum of psychiatric/neurological abnormalities ranging from subclinical alterations to coma".[1] Epidemiological reports suggest that majority of patients with cirrhosis develop HE at some point of time during the course of the disease. Approximately 30 to 50 % of cirrhotic patients develop overt HE and 10 to 50% of them develop minimal HE. Moreover, cirrhotic patients suffering from HE have a poor survival rate i.e., 42% after one year and 23% after three years of follow-up.[2]

Hyperammonemia is considered as key contributor in the pathogenesis of HE.[3] Studies have reported the direct effects of ammonia on the cerebral energy metabolism affecting glycolysis, tricarboxylic acid (TCA) cycle and electron transport chain.[4] Energy failure appears to be an important pathogenetic component in HE. Although, disturbance in energy metabolism in HE was proposed for the first time in 1955 by Bessman and Bessman yet the role of cerebral energy metabolism in the development of chronic HE needs to be elucidated for understanding pathogenesis and prognosis. Cerebral energy metabolism has also been reported to be impaired in rodent model of HE.[5] In brain, ammonia is metabolised to glutamine in astrocytes that impairs energy metabolism at various loci.[6,7] Increase in glutamine levels that contributes to astrocyte swelling, which results in brain edema.[8] Wang et al. observed increase in glutamine and branched chain amino acids (BCAAs) in human astrocytes treated with ammonium chloride.[9] The role of cerebral energy deficits in the development of HE has been shown in terms of activation of cerebral AMP-activated protein kinase, a major energy sensor in the cell, as a compensatory response to liver failure following bile duct ligation, BDL.[10] Furthermore, several studies have examined disturbances in energy metabolism in HE either in patients[11] or in animal models of HE and findings are incoherent. Hawkins and Jessy have reported decrease in cerebral metabolic rate for glucose (CMRglc) in portacaval-shunted rats[12], while studies by Cruz and Duffy found increase in CMRglc[13], whereas no change has been reported in hyperammonemic rats.[14]

Metabolomics analyses all low-molecular weight metabolites and examines metabolic changes in various disease conditions and thus provides snapshot of functional endpoint of complete biological network and best describes the cellular activity and physiological state.[15] It has already been successfully applied to highlight disease biomarkers in multiple medical fields.[16] Moreover, metabolomics approach was also used to study the regional brain metabolic patterns in a variety of biological samples such as tissue extracts and bio-fluids.[17,18] Nuclear

magnetic resonance (NMR) spectroscopy is used to detect a series of cerebral metabolites involving energy metabolism, neurotransmitters, membrane metabolism as well as antioxidants and osmolytes.[19,20] NMR based metabolomics is preferred as routine identification of disease specific biomarkers as it requires less time and little sample preparation.[21] Moreover, it is particularly useful to detect compounds that are less tractable to other analytical methods used in metabolomics such as sugars and other highly polar compounds.[22] Though, various metabolites have been analysed in experimental model of HE and in body fluids of patients with HE, however none of the study provides global picture of pathways involved in liver and brain in HE. Therefore, the present study was designed to assess metabolic profiling of liver and brain by high-field NMR spectroscopy and subsequent multivariate analyses to characterize metabolic perturbations associated with HE along with histological and neurobehavioural changes.

Materials and Methods

Chemicals

Deutrated oxide (^2H_2O) used for NMR was purchased from Sigma Aldrich (St. Louis, MO, USA). Methanol and chloroform were of HPLC grade and purchased from Sisco Research Laboratories (SRL) Pvt. Ltd. (Mumbai, India). Absorbable surgical sutures for surgery were purchased from Johnson & Johnson Pvt. Ltd. (Mumbai, India). All other chemicals used in this study were of analytical grade.

Animals and Treatment Schedule

Male Wistar rats weighing between 220 and 250 g were obtained from the Central Animal House, Panjab University, Chandigarh, India. The animals were allowed to acclimatize to the local vivarium for atleast a week prior to the use in study. All the experimental protocols were approved by the Institutional Animal Ethics Committee and were in accordance with the guidelines for humane use and care of laboratory animals *(IAEC Approval No: PU/45/99/CPCSEA/IAEC/2018/107)*. The study was planned for duration of 3 weeks. The animals were randomly segregated into following two groups with each group having six animals:

- Sham control (SC): animals underwent laparotomy without BDL
- BDL: Animals in this group underwent BDL surgery

BDL Surgery

Laparotomy was performed under general anesthesia using a mixture of ketamine (100 mg/kg) and xylazine (10 mg/kg). The sham operation consisted of a laparotomy and bile duct identification without ligation. In the BDL rats, bile duct was carefully isolated, doubly ligated using suture and then cut between these two ligatures. The abdominal incision was closed with absorbable suture (2-0) and the skin incision was closed with normal suture. The body temperature of animal was maintained at 37 ± 1^{o}C during the entire surgical procedure. The rats were then allowed to recover with free access to chow and water.

Liver function tests

Assays for alkaline phosphatase (ALP), bilirubin and cholesterol were performed in serum and plasma using commercially available kits (RECKON, manufactured by reckon diagnostic pvt. Ltd.).

^{1}H NMR based metabolic profiling

Sample preparation: The tissues (liver, cortex and hippocampus) excised immediately after animal sacrifice, were precisely weighed, flash frozen in liquid N_2 and stored at -80°C until further use. The frozen tissue samples were finely grinded in liquid nitrogen using pre-cooled pestle and mortar. The methanol-chloroform-water extraction procedure was used for metabolites extraction from the grinded tissue samples as described by Beckonert et al. (2010) with some modifications. Briefly, the grinded tissue sample was mixed with 4 ml of chloroform: methanol (1:1 v/v) and vortexed for 1 minute. The mixture was then kept at -20°C for 30 minutes to precipitate the proteins. Then, 2 ml of ice-cold distilled water was added to it and centrifuged at 10,000×g for 15 minutes. The lower organic phase (chloroform) and upper aqueous phase (methanol/water) were clearly separated by an insoluble interface. The aqueous and organic phases were transferred by pipetting to separate vials. The aqueous phase was freeze-dried and reconstituted in 750 µl of deuterium oxide ($^{2}H_2O$), containing 200 mM phosphate buffer solution (pH=7.4) and 0.5 mM sodium (3-trimethylsilyl)-2,2,3, 3-tetradeuteriopropionate (TSP), used for internal referene in the NMR specta. The aqueous phase was then transferred into a 5-mm NMR tube for NMR measurements.

^{1}H NMR Spectroscopy: The ^{1}H NMR spectra of all tissue samples were acquired on a Biospin Avance-III 800 MHz NMR spectrometer operating at 800.21 MHz equipped with crogenic probehead and a temperature of 300 °K. For each sample, one-dimensional ^{1}H-NMR spectra were recorded using the Carr–Purcell–Meiboom–Gill (CPMG) pulse sequence (cpmgpr1d, standard Bruker pulse program) with presaturation of the water peak. All the spectra were

processed using Topspin2.1 (Bruker NMR data Processing Software) using standard Fourier Transformation (FT) procedure followed by manual phase and baseline-correction. The internal standard, TSP was used for chemical shift referencing of its protons at 0 ppm. The intensity of the TSP peak was used to determine the relative concentration of each metabolite. The spectral analysis and metabolite signal integration was carried out using the ACD NMR processor software (Advanced Chemistry Development Inc., Toronto, Canada). The ^{1}H-NMR peaks for each metabolite was identified using Human Metabolome Database (HMDB) and data obtained from various research papers.[22,23,24,25] All assigned values were then subjected to multivariate statistical analysis to identify the altered metabolic pattern.

Histological Staining

The animals were anaesthetized and transcardially perfused with phosphate buffer saline (PBS) (pH 7.4, 0.1 M) followed by fixation with 4% paraformaldehyde. Brain and liver samples were post-fixed in 4% formalin prepared in PBS for 24 hours. Fixed tissues were dehydrated in various grades of alcohol and cleared in benzene. Tissues were removed; transverse sections were embedded in molten paraffin wax and sections of 5 microns thickness were cut using a microtome. Brain sections were stained with hematoxylin and eosin (H & E) for detection of necrosis.[26] The number of pyknotic cells/field was analyzed using ImageJ software (NIH, Bethesda, MD, USA). Liver samples were stained with Sirius Red (SR) and Masson Trichome (MT) to assess liver fibrosis. The percentage of SR and MT stained sections in the portal areas of liver tissue were measured using ImageJ software (NIH, Bethesda, MD, USA).

Neurobehavioral studies

Each animal was subjected to a set of neurobehavioral tests for learning, memory, anxiety and depression.

Morris water maze test: Spatial learning and memory of the animals were assessed by Morris water maze test.[27] The maze consisted of a circular water tank (140 cm in diameter and 60 cm in height) with water maintained at 25± 2°C and at a level of 40 cm above the floor of tank. A plexiglass platform invisible to the rats was placed 2 cm below the water level inside the tank. During the training session, each rat was placed at starting point of all four quadrants randomly. During the test, rat placed at starting point of one of the four quadrants had to escape to the platform submerged underneath the water. The rat was allowed to remain on the

platform for 20 seconds before the commencement of the next trial. The rat was guided to the platform if it could not reach the platform within the maximum allowed time of 180 seconds. The time taken (escape latency) and distance travelled to reach the platform was recorded at day 0 (before BDL), 14, and 21 post BDL surgery using ANY-maze TMvideo tracking software (Stoelting, Wood Dale, IL, USA).

A probe trial was performed on day 22 of the BDL surgery, wherein the extent of memory retrieval was assessed as described by Vorhees and Williams. In the probe trial test hidden plexiglass platform was removed from the pool and rats were allowed to explore the maze for 180 seconds. Various parameters including time spent, number of entries and distance travelled in the quadrant containing platform were recorded.

Open field test: The open field test provides simultaneous measures of locomotion, exploration and anxiety.[28] The open field apparatus consisted of black plywood chamber (72 cm x 72 cm with 36 cm walls). Each animal was allowed to spend 5 minutes in the apparatus and the parameters such as total distance travelled and total time (mobile) were used for the measurement of locomotion. The number of central square entries and rearing frequency were used as measures of anxiety.

Sucrose Preference test: Depression-like-symptoms viz. anhedonia (inability to feel pleasure in normal pleasurable activities) were evaluated using sucrose preference test (SPT). The rodents have an inherent interest for sweet foods or solutions.[29] Reduced preference for sweet represents anhedonia. SPT was performed in the home cage. The rats were presented with two bottles one contained normal drinking water and second contained 2% (w/v) sucrose solution. The water and sucrose intake was measured daily for 3 days and the position of two bottles were reversed to reduce any side bias. Prior to begin the test, the rats were habituated to two drinking bottles for at least 3 days. After habituation, the rats were separated with single animal per cage and presented with two drinking bottles. Sucrose preference was calculated as a percentage of the volume of sucrose intake over the total volume of water intake and averaged over the 3 days of testing.[30]

$$Sucrose\ Preference\ = \frac{Volume\ (Sucrose\ solution)}{Volume\ (Sucrose\ solution) + \ Volume\ (Water)} \times 100$$

Statistical Analysis

The data is expressed as mean ± standard error mean (SEM) and analyzed using independent t-test between the groups to analyse behavioural and histological parameters.

Values with $p < 0.05$ were considered as statistically significant. The ^{1}H NMR spectral data were converted to comma-separated values (CSV) format using Microsoft excel and imported into MetaboAnalyst3.0 for multivariate analysis. Initially, principal component analysis (PCA) was applied to identify the clustering patterns and outliers. Partial least squares discrimination analysis (PLS-DA) was used for pattern recognition analysis and isolating significant metabolites based on their PLS-DA, variable influence on projection (VIP) and coefficient scores. PLS-DA model was validated by 10-fold cross validation method by describing R^2 and Q^2 values. R^2 indicates goodness of fit and the predictive capability while $Q^2 > 0.5$ indicate that the models possessed a satisfactory fit with good predictive power. Two-tailed Pearson's correlation and regression analyses were performed to find the relation between the metabolic profiles of cortex and hippocampus with the neurobehavioural parameters.

Results

Liver function tests

Table 1 depicts the activity of ALP and levels of bilirubin, and cholesterol. The serum levels of total, direct (conjugated), and indirect (unconjugated) bilirubin showed 21-, 25- and 19-fold increase in BDL rats. The activity of ALP enzyme in serum was significantly increased in BDL rats by 2-fold. An increase by 2-fold was also observed in cholesterol level in the case of BDL rats compared to the sham controls. Thus, these results reflect the impairment in liver functions induced by the BDL.

Metabolic profiling

Metabolic alterations in liver:

A typical 1D ^{1}H NMR spectra of the aqueous phase from liver of SC and BDL animals is shown in **Figure 1.** The NMR spectra reveal signals mainly from amino acids (e.g. leucine, isoleucine, valine, arginine, lysine, proline, glutamate, methionine, glycine, tyrosine and phenylalanine). Other identified metabolites were lactate, acetate, succinate, creatine, choline, betaine, glucose, taurine and pyridoxine. All these metabolites are shown in **Table 2** with their chemical shift values and VIP scores. Out of many altered metabolites, the mean concentration of glucose, phenylalanine and pyridoxine were significantly decreased, while BCAAs (isoleucine, leucine, and valine), lactate, arginine, glutamate, succinate, methionine, creatine, tyrosine, antioxidants and/or osmolytes (betaine, choline, taurine and glycine) were

significantly increased. These differentially expressed metabolites were mapped to amino acid metabolism, Krebs cycle and glycolysis pathway as depicted in **Figure 3A**.

Metabolic alterations in brain:

Figure 1 illustrates ^{1}H NMR spectrum of the aqueous phase from the cortex of SC and BDL animals. In cortex, the mean concentration of propylene glycol, methylmalonate, creatine, choline, taurine, glucose and myo-inositol were significantly decreased, while neurotransmitters (N-acetylglutamate/N-acetylaspartate (NAA/NAG), glutamate, 4-aminobutyrate, and glutamine), TCA cycle intermediates (succinate, citrate and malate), acetate, glycine and lactate were significantly increased in BDL animals. All these metabolites were shown in **Table 3** with their chemical shift values and VIP scores.

^{1}H NMR spectra of hippocampus obtained from SC and BDL animals are shown in **Figure 1.** In hippocampus, the mean concentration of amino acids (isoleucine, alanine, proline and leucine), propylene glycol, malate (TCA cycle intermediate), creatine, antioxidants and/or osmolytes (choline, betaine and taurine), glucose and myo-inositol were significantly decreased, while methylmalonate, acetate, neurotransmitters (NAA/NAG, glutamate, 4-aminobutyrate, glutamine), TCA cycle intermediates (succinate and citrate), amino acids (aspartate, glycine and tyrosine), methanol and lactate were significantly increased in BDL animals as compared to SC. All these metabolites were shown in **Table 4** with their chemical shift values and VIP scores. Thus, the metabolites responsible for separating BDL group from control included alterations in neurotransmission and energy metabolic pathways in **Figure 3B**.

Multivariate analysis

The unsupervised PCA of the metabolite data from all samples revealed the general structure of the complete data set. In PCA plots, the samples with similar metabolic profile grouped together while the samples with altered metabolism were found to be dispersed **(Figure 2).** The HE group showed considerable difference from the control group by increased PC2 scores and decreased PC1 scores in liver. In cortex, control and HE groups reflected similar metabolic profiles while, in hippocampus, HE group showed considerable difference from the control group by increased PC2 scores. Thus, as a result, PC2 appears to be responsible for the separation between control and HE groups in liver and hippocampus. PLS-DA was applied to obtain an overview of the complete data set and discriminate the variables that are responsible for variation between the groups to identify features with

discriminative power. The quality and reliability of the PLS-A models were validated based on R^2 and Q^2 values derived using 10-fold cross validation algorithm. The R^2 and Q^2 values in the Figure 2 alluded that the PLS-DA models possessed satisfactory fit with good predictive power. These results indicate that the established PLS-DA model is reliable and good in classifying and discriminating between SC and the BDL group. The differential metabolites were selected based on the statistically significant threshold of VIP values (i.e., ≥1.0) obtained from the PLS-DA model and PLS-DA coefficients score (i.e., >30% in the present study). The coefficient importance is based on the weighted sum of PLS regression scores; whereas the VIP score represents a weighted sum of squares of the PLS loadings and takes into account the amount of explained Y variation in each dimension to measure the impact of each metabolite in the model. The VIP criterion indirectly imitates the correlation of the metabolites with disease and is an extensively used method for biomarker selection. In addition, the permutation test plots showed that the Q2 regression line had a negative intercept and all of the permutated R2 and Q2 values to the left were lower than the original points to the right **(Figure 2)**, which indicated that the models in the present study are valid.

Histopathological changes in liver

Sirius red staining revealed a significant increase in the collagen content, typical perisinusoidal, periportal, and peribiliary fibrosis, resulting in the formation of fibrotic septae and deposition of extra cellular matrix in BDL rats three weeks after the surgery **(Figure 4)**. Moreover, percentage of Sirius red stained area was significantly higher in the BDL rats as compared to SC rats **(Figure 4C).** Furthermore, Masson trichome stain also revealed severe liver injury that included cellular destruction, infiltration of lymphocytes and visible collagen accumulation in the BDL animals as compared to sham controls **(Figure 4E).** The Masson trichrome stained area (blue) was significantly higher in BDL rats as compared to SC rats **(Figure 4F)**. Liver of sham controls showed a normal morphology with intact hepatocytes and portal tracts **(Figure 4A&D).** Liver of BDL rats showed biliary fibrosis accompanied by loss of hepatic structure **(Figure 4B&E).**

Histopathological changes in Brain

In brain, H & E staining of cortex and hippocampus sections of BDL rats showed marked increase in neuronal degeneration, pyknotic and shrunken neurons as compared to SC rats **(Figure 4G, H, I &J)**

Neurobehaviour tests

Morris water maze:

A significant increase was observed in the distance travelled (5.1 fold) and total time taken (11.6 fold) by the BDL rats to reach the quadrant containing the platform (Descent latency) as compared to the SC rats on day 21 post BDL **(Figure 5B & C)**. This was also evident from the track plot reports wherein the track lines reflect the path followed by the animal to locate the hidden platform **(Figure 5A).** In the memory retrieval test performed on day 22, a significant decline was observed in the number of entries (42%), time spent (48%) and distance travelled (37%) by the BDL rats in the quadrant containing platform as compared to SC rats **(Table 5).** This suggested impaired learning and memory in BDL rats. Further, **Table 6.1 and 6.2** summarizes Pearson correlation between metabolic profile of cortex and hippocampus with the behavioural parameters. Interestingly, we observed a significant correlation between descent latency and NAA/choline (Cortex: $r= 0.68, p<0.05$; Hippocampus: $r= 0.69, p<0.05$, **Figure 8A**), descent latency and choline/creatine (Cortex: $r= - 0.65, p<0.05$; Hippocampus: $r= - 0.67, p<0.05$, **Figure 8B**), descent latency and NAA/creatine (Cortex: $r= 0.75, p<0.05$; Hippocampus: $r = 0.70, p<0.05$, **Figure 8C)**.

Open field test:

Locomotion and anxiety like behaviour evaluated using open field test showed significant decline in total distance travelled (3.5 fold) and mobility time (3.3 fold) by the animals that underwent BDL surgery as compared to SC **(Figure 6B & C).** However, a significant decrease was also observed in the frequency of entries to the central zone (5.1 fold) and frequency of rearing (4.2 fold) on day 21 post surgery as compared to SC **(Figure 6D & E)**. This was also evident from the track plot that reflects the path followed by the animal during exploration **(Figure 6A).** Thus, the BDL animals showed reduced locomotion and increased anxiety like behaviour. Further, there was a significant correlation between total distance travelled and NAA/choline (Cortex: $r = - 0.67, p<0.05$; Hippocampus: $r = - 0.64, p<0.05$, **Figure 9A**), total distance travelled and choline/creatine (Cortex: $r = 0.62, p<0.05$; Hippocampus: $r = 0.64, p<0.05$, **Figure 9B**), total distance travelled and NAA/creatine (Cortex: $r = - 0.67, p<0.05$; Hippocampus: $r = - 0.64, p<0.05$, **Figure 9C)**. Moreover, **Table 6.1 and 6.2** summarizes the pearson correlation of all the metabolites with the time animal was mobile and total distance travelled.

Sucrose preference test:

Depression like behaviour was assessed in terms of intake of sucrose over water which was measured for 3 days post surgery. **Figure 7** depicts that BDL rats exhibited a 78 % decrease in sucrose preference as compared to SC. BDL rats exhibited decreased ability to experience pleasure and thus showing depressive like behaviour. Further, the depressive-like behaviour was correlated with the metabolic profiles of cortex and hippocampus **(Table 6.1 and 6.2)**.

Discussion

Hepatic encephalopathy is a well known complication of liver cirrhosis. The animal model that is particularly useful for the study of HE is the bile duct ligation (BDL) model. Various studies have reported increase in the ammonia levels following BDL. This model is also associated with elevated liver enzymes, increase in hepatic collagen and hydroxyproline content leading to the development of liver fibrosis in rats.[31] Similarly, in the present study, increased activity of ALP, bilirubin and cholesterol were observed in BDL animals as compared to control. The histological staining of liver showed deposition of collagen and loss of hepatic structure in BDL animals. Since, HE is an inter-organ disease that triggers a pathophysiological cascade of events affecting other organs that results in changes at the metabolic level. These changes often show their manifestations in term of presence, absence or altered concentration of the affected metabolite(s), in the bio fluids and tissues. Here, the present study reveals metabolic perturbations in response to HE using ^{1}H NMR based metabolomics.

Analysis of ^{1}H NMR metabolic profiles of both liver and brain from sham control versus BDL group revealed clear differences that were rapidly characterized using multivariate statistical approaches. The major metabolic disturbance detected in the liver of BDL rats includes increased levels of lactate and decreased levels of glucose. Decreased glucose levels reflect either impairment in glucose uptake or increased rate of glucose metabolisation. Increase in the rate of glycolysis is a well-known phenomenon in acute and chronic HE and hyperammonemia.[32] Increased lactate levels in liver suggest that pyruvate generated in glycolysis was converted to lactate, instead of being channelled to TCA cycle. Similarly, in low or chronic alcohol consumption, excess lactic acid is transported from the liver to peripheral tissues, where energy level is lower, and lactic acid may be reconverted to pyruvic acid for metabolic needs. Moreover, it is reported that in acute alcohol consumption, TCA cycle is known to be inhibited[33], which was also indicated in our study by the increased levels of TCA cycle intermediate such as succinate and glutamate. Glutamate, the precursor

of glutamine is the most abundant amino acids involved in nitrogen metabolism. Glutamine enters into the TCA cycle following its deamination into ketoglutarate. In other liver pathologies such as hepatocellular carcinoma, hepatic transplantation failure and fulminant hepatitis, the levels of glutamine were found to be increased in plasma, serum as well as in urine.[34,35,36]

The amino acids are also detectable in liver that mainly includes BCAAs such as valine, leucine and isoleucine, which serve as a substrate for protein synthesis, glyconeogenesis and act as a precursor for various hormones. The increased levels of free BCAAs in the liver of BDL rats reflected increased degradation of proteins and the higher release of these amino acids by the liver. Muscles along with liver release a high quantity of amino acids present in the body to maintain cellular homeostasis in condition of energy deprivation.[37] Additionally, increased levels of arginine were observed in liver of BDL group. This increase in arginine causes the increase in proline production and proline is responsible for the deposition of collagen in the liver.[38] Increased collagen content in liver has also been shown by histopathological staining with sirius red and masson trichome Increased collagen correlated with the increase in the free proline was also evident in experimental fibrosis[39] and human cirrhosis.[40]

In brain, increased lactate and decreased glucose levels in BDL animals indicates impaired aerobic glycolysis and TCA cycle and thus dampened the ATP production. These results are consistent with the previous reports in patients with HE and hyperammonemia as well as in animals with acute liver failure.[41,42,43,44] Amino acids serve as a key source of energy, especially during conditions in which glucose availability is limited. The levels of BCAAs including isoleucine and leucine were found to be low in the brain of BDL rats. Isoleucine and leucine are ketogenic amino acids and as the levels of acetate were increased so it might be an index of ketogenesis in encephalopathy. Moreover, the major change found in brain involves alterations in neurotransmitter levels. Glutamate is the main excitatory neurotransmitter of the central nervous system. The levels of glutamate, glutamine and 4-aminobutyrate (GABA) were increased in BDL rats as compared to control. Montana et al. also observed increased glutamate release from astrocytes in HE.[45] The glutamine/glutamate (Gln/Glu)- GABA cycle (GGC) between astrocytes and neurons has been known to be the brain's primary mechanism for ammonia detoxification. Disturbance in GGC in brain results in hyperammonemia which leads to cognitive and motor impairments. These findings were further supported by the neurobehavioral tests which revealed significant impairment in cognition and motor functions. Memory and learning impairment during HE was assessed by

morris water maze test, which showed a progressive increase in the transfer latency and the distance travelled to reach the hidden platform from day 14 onwards to day 21 suggesting impaired memory acquisition. Similarly, Huang et al. have shown that swim length used as a measure of spatial memory, was higher in case of BDL rats as compared to SC rats.[46] Memory and learning impairment during HE can also be linked with the decreased levels of choline in brain as cholinergic system has been shown to be associated with memory.[47] Choline is responsible for the formation of important neurotransmitter: acetylcholine and two major phospholipids: phosphatidylcholine and sphingomyelin. Studies have shown that decreased levels of choline and acetylcholine in the hippocampus and adjacent cortical areas produces memory loss comparable to anterograde amnesia.[48] Choline and myo-inositol are considered important osmolytes in astrocytes.[49] In the present study, decreased levels of both were found in the brain which reflects increased cell swelling that may leads to brain edema. Brain edema is one of the pathological conditions in HE patients.[50] A decreased levels are also observed in acute liver failure and HE patients[51] which is similar to what is seen in our results. Furthermore, we have also found a significant correlation between NAA/Choline and Choline/Creatine ratio with the descent latency and total distance travelled, indicating a specific metabolic link with cognitive and motor impairments following BDL. Similarly, Ben Salem et al also reported NAA/Creatine and Choline/Creatine ratios as a marker of cognitive impairment in the elderly population.[52]

The alterations in neurotransmitter levels in brain reflect the behavioural impairemt in BDL rats. These behavioural changes are of interest as it is well known that patients with chronic HE exhibit impaired Cognitive and motor functions. Anxiety and depression are also the most common symptoms in HE.[53] In the present study, BDL rats have shown a decrease in locomotor and exploratory activity while undergoing the open field behavioural task.. Depressive like behaviour was also shown by the BDL rats as assessed by sucrose preference test. Similarly, Jiang et al. showed that BDL surgery induced a significantly reduced sucrose preference in rats, while the indoleamine-2,3-dioxygenase (IDO) inhibitor 1-MT treatment reversed this decrease, indicating depression is accompanied by HE.[54]

In conclusion, our results indicated significant dysregulation of metabolic pathways in both liver and brain. The metabolic alterations were associated with the disturbance of energy metabolism (glycolysis, TCA cycle and ketogenesis), amino acid metabolism and neurotransmission in brain. Additionally, BDL induced neurobehavioral abnormalities appear to result from altered energy metabolism and neurotransmitter levels, which were observed in

both cortex and hippocampus. Thus, the combination of these metabolic alterations may hold promise for early prediction and development of better prognostic markers.

Acknowledgements

The financial assistance provided by the Department of Science and Technology (DST), New Delhi under Promotion of University Research and Scientific Excellence (PURSE) grant and the University Grants Commission (UGC), New Delhi under the Basic Science Research (BSR) and UGC-Special Assistance Programme (UGC-SAP) is acknowledged. We also acknowledge the High Field NMR Facility at Centre of Biomedical Research (CBMR), Lucknow, India for NMR data acquisition.

Conflict of Interest

The authors declare no competing conflict of interest

References

(1) Vilstrup, H.; Amodio, P.; Bajaj, J.; Cordoba, J.; Ferenci, P.; Mullen, K. D.; Weissenborn, K.; Wong, P.; Talwalkar, J. A.; Conjeevaram, H. S.; Porayko, M.; Merriman, R. B.; Jansen, P. L. M.; Zoulim, F. Hepatic Encephalopathy in Chronic Liver Disease: 2014 Practice Guideline by the European Association for the Study of the Liver and the American Association for the Study of Liver Diseases. *J. Hepatol.* **2014**, *61*, 642–659.

(2) Poordad, F. F. Review Article: The Burden of Hepatic Encephalopathy. *Aliment. Pharmacol. Ther.* **2007**, *25*, 3–9.

(3) Jayakumar, A. R.; Norenberg, M. D. Hyperammonemia in Hepatic Encephalopathy. *Journal of Clinical and Experimental Hepatology*. **2018**, *8*, 272–280.

(4) Rama Rao, K. V.; Norenberg, M. D. Brain Energy Metabolism and Mitochondrial Dysfunction in Acute and Chronic Hepatic Encephalopathy. *Neurochemistry International*. **2012**, *60*, 697–706.

(5) Dhanda, S.; Sunkaria, A.; Halder, A.; Sandhir, R. Mitochondrial Dysfunctions Contribute to Energy Deficits in Rodent Model of Hepatic Encephalopathy. *Metab. Brain Dis.* **2018**, *33*, 209–223.

(6) Cooper, A. J. L.; Jeitner, T. M. Central Role of Glutamate Metabolism in the Maintenance of Nitrogen Homeostasis in Normal and Hyperammonemic Brain. *Biomolecules*. **2016**, *6*, 16.

(7) Cruzat, V.; Rogero, M. M.; Keane, K. N.; Curi, R.; Newsholme, P. Glutamine: Metabolism and Immune Function, Supplementation and Clinical Translation. *Nutrients*. **2018**, *10*, 1564.

(8) Jayakumar, A. R.; Rao, K. V. R.; Murthy, C. R. K.; Norenberg, M. D. Glutamine in the Mechanism of Ammonia-Induced Astrocyte Swelling. *Neurochem. Int.* **2006**, *48*, 623–628.

(9) Wang, T.; Suzuki, K.; Kakisaka, K.; Onodera, M.; Sawara, K.; Takikawa, Y. L-carnitine Prevents Ammonia-induced Cytotoxicity and Disturbances in Intracellular Amino Acid Levels in Human Astrocytes. *J. Gastroenterol. Hepatol.* **2019**, *34*, 1249–1255.

(10) Dagon, Y.; Avraham, Y.; Ilan, Y.; Mechoulam, R.; Berry, E. M. Cannabinoids Ameliorate Cerebral Dysfunction Following Liver Failure via AMP-Activated Protein Kinase. *FASEB J.* **2007**, *21*, 2431-41.

(11) Strauss, G. I.; Møller, K.; Larsen, F. S.; Kondrup, J.; Knudsen, G. M. Cerebral Glucose and Oxygen Metabolism in Patients with Fulminant Hepatic Failure. *Liver Transplant.* **2003**, *9*, 1244–1252.

(12) Hawkins, R. A.; Jessy, J. Hyperammonaemia Does Not Impair Brain Function in the Absence of Net Glutamine Synthesis. *Biochem. J.* **1991**, *277*, 697–703.

(13) Cruz, N. F.; Duffy, T. E. Local Cerebral Glucose Metabolism in Rats with Chronic Portacaval Shunts. *J. Cereb. Blood Flow Metab.* **1983**, *3*, 311–320.

(14) Cruz, N. F.; Dienel, G. A. Brain Glucose Levels in Portacaval-Shunted Rats with Chronic, Moderate Hyperammonemia: Implications for Determination of Local Cerebral Glucose Utilization. *J. Cereb. Blood Flow Metab.* **1994**, *14*, 113–124.

(15) Peng, B.; Li, H.; Peng, X. X. Functional Metabolomics: From Biomarker Discovery to Metabolome Reprogramming. *Protein and Cell*. **2015**, *6*, 628–637.

(16) Beckonert, O.; Coen, M.; Keun, H. C.; Wang, Y.; Ebbels, T. M. D.; Holmes, E.; Lindon, J. C.; Nicholson, J. K. High-Resolution Magic-Angle-Spinning NMR Spectroscopy for Metabolic Profiling of Intact Tissues. *Nat. Protoc.* **2010**, *5*, 1019–1032.

(17) Ivanisevic, J.; Siuzdak, G. The Role of Metabolomics in Brain Metabolism Research. *J. Neuroimmune Pharmacol.* **2015**, *10*, 391–395.

(18) Ivanisevic, J.; Epstein, A. A.; Kurczy, M. E.; Benton, P. H.; Uritboonthai, W.; Fox, H. S.; Boska, M. D.; Gendelman, H. E.; Siuzdak, G. Brain Region Mapping Using Global Metabolomics. *Chem. Biol.* **2014**, *21*, 1575–1584.

(19) Duarte, J. M. N.; Lei, H.; Mlynárik, V.; Gruetter, R. The Neurochemical Profile Quantified by in Vivo 1H NMR Spectroscopy. *NeuroImage*. **2012**, *61*, 342-62.

(20) Zheng, H.; Zhao, L.; Xia, H.; Xu, C.; Wang, D.; Liu, K.; Lin, L.; Li, X.; Yan, Z.; Gao, H. NMR-Based Metabolomics Reveal a Recovery from Metabolic Changes in the Striatum of 6-OHDA-Induced Rats Treated with Basic Fibroblast Growth Factor. *Mol. Neurobiol.* **2016**, *53*, 6690–6697.

(21) Emwas, A. H.; Roy, R.; McKay, R. T.; Tenori, L.; Saccenti, E.; Nagana Gowda, G. A.; Raftery, D.; Alahmari, F.; Jaremko, L.; Jaremko, M.; Wishart, D. S. Nmr Spectroscopy for Metabolomics Research. *Metabolites*. **2019**, *9*, 9-123.

(22) Amathieu, R.; Triba, M. N.; Nahon, P.; Bouchemal, N.; Kamoun, W.; Haouache, H.; Trinchet, J.-C.; Savarin, P.; Le Moyec, L.; Dhonneur, G. Serum 1H-NMR Metabolomic Fingerprints of Acute-On-Chronic Liver Failure in Intensive Care Unit Patients with Alcoholic Cirrhosis. *PLoS One* **2014**, *9*, e89230.

(23) Wishart, D. S.; Tzur, D.; Knox, C.; Eisner, R.; Guo, A. C.; Young, N.; Cheng, D.; Jewell, K.; Arndt, D.; Sawhney, S.; Fung, C.; Nikolai, L.; Lewis, M.; Coutouly, M.-A.; Forsythe, I.; Tang, P.; Shrivastava, S.; Jeroncic, K.; Stothard, P.; Amegbey, G.; Block, D.; Hau, D. D.; Wagner, J.; Miniaci, J.; Clements, M.; Gebremedhin, M.; Guo, N.; Zhang, Y.; Duggan, G. E.; MacInnis, G. D.; Weljie, A. M.; Dowlatabadi, R.; Bamforth, F.; Clive, D.; Greiner, R.; Li, L.; Marrie, T.; Sykes, B. D.; Vogel, H. J.; Querengesser, L. HMDB: The Human Metabolome Database. *Nucleic Acids Res.* **2007**, *35* (Database), D521–D526.

(24) Lin, C.; Chen, Z.; Zhang, L.; Wei, Z.; Cheng, K.-K.; Liu, Y.; Shen, G.; Fan, H.; Dong, J. Deciphering the Metabolic Perturbation in Hepatic Alveolar Echinococcosis: A 1H NMR-Based Metabolomics Study. *Parasit. Vectors* **2019**, *12*, 300.

(25) McPhail, M. J. W.; Montagnese, S.; Villanova, M.; El Hadi, H.; Amodio, P.; Crossey, M. M. E.; Williams, R.; Cox, I. J.; Taylor-Robinson, S. D. Urinary Metabolic Profiling by 1H NMR Spectroscopy in Patients with Cirrhosis May Discriminate Overt but Not Covert Hepatic Encephalopathy. *Metab. Brain Dis.* **2017**, *32*, 331–341.

(26) Kmiec, Z. J.A. Kiernan. Histological and Histochemical Methods: Theory and Practice. 5th Edition, Scion Publishing, 2015, 571 Pp. *Folia Histochem. Cytobiol.* **2016**.

(27) Vorhees, C. V.; Williams, M. T. Morris Water Maze: Procedures for Assessing Spatial and Related Forms of Learning and Memory. *Nat. Protoc.* **2006**, *1*, 848–858.

(28) Walsh, R. N.; Cummins, R. A. The Open-Field Test: A Critical Review. **1976**, 482–504.

(29) Fernandez, J. W.; Grizzell, J. A.; Philpot, R. M.; Wecker, L. Postpartum Depression in Rats: Differences in Swim Test Immobility, Sucrose Preference and Nurturing Behaviors. *Behav. Brain Res.* **2014**, *1*, 75–82.

(30) Serchov, T.; van Calker, D.; Biber, K. Sucrose Preference Test to Measure Anhedonic Behaviour in Mice. *Bio-Protocol* **2016**, *6*, 5–8.

(31) Dhanda, S.; Kaur, S.; Sandhir, R. Preventive Effect of N-Acetyl-L-Cysteine on Oxidative Stress and Cognitive Impairment in Hepatic Encephalopathy Following Bile Duct Ligation. *Free Radic. Biol. Med.* **2013**, *56*, 204–215.

(32) Rao, K. V. R.; Norenberg, M. D. Cerebral Energy Metabolism in Hepatic Encephalopathy and Hyperammonemia. *Metabolic Brain Disease*. **2001**, *16*, 67–78.

(33) Irwin, C.; Van Reenen, M.; Mason, S.; Mienie, L. J.; Wevers, R. A.; Westerhuis, J. A.; Reinecke, C. J. The1H-NMR-Based Metabolite Profile of Acute Alcohol Consumption: A Metabolomics Intervention Study. *PLoS One* **2018**, *13*, e0196850..

(34) Yang, Y.; Li, C.; Nie, X.; Feng, X.; Chen, W.; Yue, Y.; Tang, H.; Deng, F. Metabonomic Studies of Human Hepatocellular Carcinoma Using High-Resolution Magic-Angle Spinning 1H NMR Spectroscopy in Conjunction with Multivariate Data Analysis. *J. Proteome Res.* **2007**, *6*, 2605–2614.

(35) Beatriz, M. G.; Morales, J. M.; Rodrigo, J. M.; Del Olmo, J.; Serra, M. A.; Ferrández, A.; Celda, B.; Monleón, D. Metabolic Profile of Chronic Liver Disease by NMR Spectroscopy of Human Biopsies. *Int. J. Mol. Med.* **2011**, *27*, 111–117.

(36) Cobbold, J. F. L.; Patel, J. H.; Goldin, R. D.; North, B. V.; Crossey, M. M. E.; Fitzpatrick, J.; Wylezinska, M.; Thomas, H. C.; Cox, I. J.; Taylor-Robinson, S. D. Hepatic Lipid Profiling in Chronic Hepatitis C: An in Vitro and in Vivo Proton Magnetic Resonance Spectroscopy Study. *J. Hepatol.* **2010**, *52*, 16–24.

(37) Evans, R. D.; Heather, L. C. Metabolic Pathways and Abnormalities. *Surgery (United Kingdom)*. **2016**, *34*, 266–272.

(38) Wu, G.; Bazer, F. W.; Burghardt, R. C.; Johnson, G. A. Proline and Hydroxyproline Metabolism: Implications for Animal and Human Nutrition. *N. Y. Times Mag.* **2010**, *40*, 42.

(39) Mann, S. W.; Fuller1, G. C.; Rodil, J. V; Vidins, E. I. Hepatic Prolyl Hydroxylase and Collagen Synthesis in Patients with Alcoholic Liver Disease. *Gut* **1979**, *20*, 825–832.

(40) Kershenobich, D.; Fierro, F. J.; Rojkind, M. The Relationship between the Free Pool of Proline and Collagen Content in Human Liver Cirrhosis. *J. Clin. Invest.* **1970**, *49*, 2246–2249.

(41) Ratnakumari, L.; Qureshi, I. A.; Butterworth, R. F. Effects of Congenital Hyperammonemia on the Cerebral and Hepatic Levels of the Intermediates of Energy Metabolism in Spf Mice. *Biochem. Biophys. Res. Commun.* **1992**, *184*, 746–751.

(42) Zwingmann, C.; Chatauret, N.; Leibfritz, D.; Butterworth, R. F. Selective Increase of Brain Lactate Synthesis in Experimental Acute Liver Failure: Results of a [1H-13C] Nuclear Magnetic Resonance Study. *Hepatology* **2003**, *37*, 420–428.

(43) Walsh, T. S.; McLellan, S.; Mackenzie, S. J.; Lee, A. Hyperlactatemia and Pulmonary Lactate Production in Patients with Fulminant Hepatic Failure. *Chest* **1999**, *116*, 471–476.

(44) Rose, C.; Ytrebø, L. M.; Davies, N. A.; Sen, S.; Nedredal, G. I.; Belanger, M.; Revhaug, A.; Jalan, R. Association of Reduced Extracellular Brain Ammonia, Lactate, and Intracranial Pressure in Pigs with Acute Liver Failure. *Hepatology* **2007**, *46*, 1883–1892.

(45) Montana, V.; Verkhratsky, A.; Parpura, V. Pathological Role for Exocytotic Glutamate

Release from Astrocytes in Hepatic Encephalopathy. *Curr. Neuropharmacol.* **2014**, *12*, 324–333.

(46) Huang, L. T.; Chen, C. C.; Sheen, J. M.; Chen, Y. J.; Hsieh, C. S.; Tain, Y. L. The Interaction between High Ammonia Diet and Bile Duct Ligation in Developing Rats: Assessment by Spatial Memory and Asymmetric Dimethylarginine. *Int. J. Dev. Neurosci.* **2010**, *28*, 169–174.

(47) García-Ayllón, M.-S.; Cauli, O.; Silveyra, M.-X.; Rodrigo, R.; Candela, A.; Compañ, A.; Jover, R.; Pérez-Mateo, M.; Martínez, S.; Felipo, V.; Sáez-Valero, J. Brain Cholinergic Impairment in Liver Failure. *Brain* **2008**, *131*, 2946–2956.

(48) Flicker, C.; Dean, R. L.; Watkins, D. L.; Fisher, S. K.; Bartus, R. T. Behavioral and Neurochemical Effects Following Neurotoxic Lesions of a Major Cholinergic Input to the Cerebral Cortex in the Rat. *Pharmacol. Biochem. Behav.* **1983**, *18*, 973–981.

(49) Videen, J. S.; Michaelis, T.; Pinto, P.; Ross, B. D. Human Cerebral Osmolytes during Chronic Hyponatremia: A Proton Magnetic Resonance Spectroscopy Study. *J. Clin. Invest.* **1995**, *95*, 788–793.

(50) Cudalbu, C.; Taylor-Robinson, S. D. Brain Edema in Chronic Hepatic Encephalopathy. *Journal of Clinical and Experimental Hepatology*. **2019**, *9*, 362–382.

(51) Gupta, R. K.; Saraswat, V. A.; Poptani, H.; Dhiman, R. K.; Kohli, A.; Gujral, R. B.; Naik, S. R. Magnetic Resonance Imaging and Localized in Vivo Proton Spectroscopy in Patients with Fulminant Hepatic Failure. *Am. J. Gastroenterol.* **1993**, *88*, 670–674.

(52) Ben Salem, D.; Walker, P. M.; Bejot, Y.; Aho, S. L.; Tavernier, B.; Rouaud, O.; Ricolfi, F.; Brunotte, F. N-Acetylaspartate/Creatine and Choline/Creatine Ratios in the Thalami, Insular Cortex and White Matter as Markers of Hypertension and Cognitive Impairment in the Elderly. *Hpertens Res*. **2008**, *31*, 1851-57.

(53) Telles-Correia, D.; João Freire, M.; Mega, I.; Barreiras, D.; Cortez Pinto, H. Anxiety and Depression Symptoms in Hepatic Encephalopathy: Are They Psychiatric or Organic? *Transplant. Proc.* **2015**, *47*, 1005–1007.

(54) Jiang, X.; Xu, L.; Tang, L.; Liu, F.; Chen, Z.; Zhang, J.; Chen, L.; Pang, C.; Yu, X. Role of the Indoleamine-2,3-Dioxygenase/Kynurenine Pathway of Tryptophan Metabolism in Behavioral Alterations in a Hepatic Encephalopathy Rat Model. *J. Neuroinflammation* **2018**, *15*, 3.

Legends to figures

Figure 1: Stack plot of representative 1D ^{1}H NMR spectra from liver, Cortex and hippocampus of SC and BDL animals.

Figure 2: Two dimensional PCA and PLS-DA score plots derived from one dimensional ^{1}H CPMG NMR spectra of liver (A, B) cortex (D, E) and hippocampus (G, H) from SC and BDL groups. Each data point denotes one subject. A 100 random permutation test for PLS-DA models generated from liver (C), cortex (F) and hippocampus (I) of control and BDL groups. The R2 value (green) represents the goodness of fit of the model. The Q2 value (blue) represents the predictability of the models.

Figure 3: Metabolic pathways related to metabolites altered in the liver (A) and brain (B) of BDL animals.

Figure 4: Photomicrographs of liver and brain sections from SC (A,D,G,I) and BDL rats (B,E,H,J) at magnification, 600X. Liver sections stained with Sirius red are shown in A and B whereas with masson trichome are reported in D and E. Arrows indicate collagen stained areas and percentage of Sirius red and masson trichome stained area analyzed using ImageJ (C and F, respectively). Cortex (G and H) and hippocampus (I and J) sections were stained with H&E. Arrows indicate pyknotic neuronal cells. Number of pyknotic cells/field analyzed using ImageJ (K). Values are expressed as mean ± SEM; n=3. *Significantly different from control group ($P<0.05$).

Figure 5: Effect of BDL on learning and memory assessed by Morris water maze test. Representative track plots of animals recorded using video tracking software ANY-maze (A) distance travelled (B) and total time (C). Values are expressed as mean ± SEM; n = 5. *Significantly different from SC group ($p < 0.05$).

Figure 6: Effect of BDL on locomotor functions assessed by open field test. Representative track plots of animals recorded using video tracking software ANY-maze (A), total distance travelled (B) time mobile (C) No. of center zone entries (D) and Rearing frequency (E). Values are expressed as mean ± SEM; n = 5. *Significantly different from SC group ($p < 0.05$).

Figure 7: Effect of BDL on depressive behavior assessed by sucrose water preference test. Values are expressed as mean ± SEM; n=5. *Significantly different from SC group ($P<0.005$).

Figure 8: Correlation plots showing the relation between cognitive behaviour with the metabolic profiles from SC and BDL. Correlation between descent latency and NAA/Choline (A), Choline/Creatine (B) and NAA/Creatine (C). Two-tailed Pearson correlation were performed.

Figure 9: Correlation plots showing the relation between Motor behavior with the metabolic profiles from SC and BDL. Correlation between total distance travelled and NAA/Choline (A), Choline/Creatine (B) and NAA/Creatine (C). Two-tailed Pearson correlation were performed.

Table 1: Effect of BDL on liver function tests.

	SC	BDL
Total bilirubin (mg/dl)	**0.31±0.03**	**6.63±1.23***
Direct bilirubin (mg/dl)	**0.13±0.02**	**3.27±0.86***
Indirect bilirubin (mg/dl)	**0.17±0.04**	**3.36±1.12***
ALP (IU/L)	**274.4±28.8**	**532.6±29.7***
Cholesterol (mg/dl)	**51.05±3.5**	**115.03±7.7***

Values are expressed as mean ±SD; *n*=5.*significantly different from control group ($P < 0.05$)

Table 2: Significant change in the metabolites derived from liver of SC and BDL animals.

Metabolite	ppm	VIP Score	Level
Isoleucine	0.93	1.0	Increase
Leucine	0.95	1.5	Increase
Valine	1.03	1.5	Increase
Lactate	1.31	4.1	Increase
Arginine	1.73	1.3	Increase
Acetate	1.91	0.5	Increase
Proline	1.99	0.6	Increase
Glutamate	2.05	1.6	Increase
Succinate	2.39	1.1	Increase
Methionine	2.63	0.9	Increase
Creatine	3.03	1.8	Increase
Tyrosine	3.07	1.8	Increase
Choline	3.19	2.8	Increase
Betaine	3.25	2.3	Increase
Glucose	3.39	3.4	Decrease
Taurine	3.43	1.9	Increase
Glycine	3.55	1.6	Increase
Lactate	4.09	1.7	Increase
Phenylalanine	7.47	1.0	Decrease
Pyridoxine	7.67	1.1	Decrease

Table 3: Significantly altered metabolites from cortex of SC and BDL animals.

Metabolite	ppm	VIP Score	Level
Propylene Glycol	1.13	1.3	Decrease
3-Hydroxyisovalerate	1.23	1.7	Increase
Methylmalonate	1.25	1.3	Decrease
Acetate	1.89	1.6	Increase
NAA/NAAG	2.01	2.1	Increase
Glutamate	2.13	4.7	Increase
4-Aminobutyrate	2.29	1.5	Increase
Succinate	2.39	2.3	Increase
Glutamine	2.45	4.1	Increase
Citrate	2.51	1.2	Increase
Malate	2.69	1.0	Increase
Creatine	3.03	1.8	Decrease
Choline	3.19	1.9	Decrease
Taurine	3.41	1.3	Decrease
Glucose	3.53	2.2	Decrease
Glycine	3.55	1.7	Increase
Myo-Inositol	3.61	1.8	Decrease
Lactate	4.09	1.0	Increase

Table 4: Significantly altered metabolites from Hippocampus of SC and BDL animals.

Metabolite	ppm	VIP Score	Level
Isoleucine	0.93	1.0	Decrease
Leucine	0.95	1.1	Decrease
Propylene Glycol	1.13	1.3	Decrease
3-Hydroxyisovalerate	1.23	2.1	Increase
Methylmalonate	1.25	2.4	Increase
Alanine	1.45	1.0	Decrease
Acetate	1.89	1.8	Increase
Proline	1.99	1.5	Decrease
NAA/NAAG	2.01	1.1	Increase
Glutamate	2.03	1.3	Increase
4-Aminobutyrate	2.29	1.7	Increase
Succinate	2.39	3.3	Increase
Glutamine	2.45	4.0	Increase
Citrate	2.51	1.7	Increase
Malate	2.69	1.1	Decrease
Aspartate	2.79	1.2	Increase
Creatine	3.03	1.4	Decrease
Choline	3.19	2.7	Decrease
Glucose	3.23	1.5	Decrease
Betaine	3.25	1.8	Decrease
Methanol	3.35	2.4	Increase
Taurine	3.41	1.4	Decrease
Glycine	3.55	2.5	Increase
Myo-Inositol	3.61	2.7	Decrease
Lactate	4.07	1.6	Increase
Tyrosine	6.89	1.0	Increase

Table 5: Probe trial activity assessed by Morris water maze in SC and BDL animals.

	SC	BDL
Number of Entries in the Quadrant Containing Platform	**23.33 ± 2.02**	**13.67 ± 2.34***
Time Spent in the Quadrant containing Platform (Seconds)	**88.66 ± 4.63**	**45.94 ± 5.20***
Distance Travelled in the Quadrant Containing platform (m)	**39.67 ± 2.42**	**25.09 ± 1.50***

Values are expressed as mean ±SD; *n*=5.*significantly different from control group ($P < 0.05$)

Table 6.1: Tabulated summary of Pearson correlation coefficients (r) between metabolic profile of cortex and the behavioural parameters.

	Metabolites	Behavioural Parameters			
		Descent Latency	Time mobile	Total distance travelled	Sucrose preference
1	Propylene Glycol	- 0.49	0.69*	0.71*	0.47
2	3-Hydroxyisovalerate	- 0.35	0.22	0.24	0.32
3	Methylmalonate	- 0.64*	0.53	0.54	0.65*
4	Acetate	0.72*	- 0.72*	- 0.76**	- 0.59
5	NAA/NAAG	0.53	- 0.43	- 0.34	- 0.49
6	Glutamate	0.55	- 0.48	- 0.45	- 0.33
7	4-Aminobutyrate	0.65*	- 0.64*	- 0.69*	- 0.51
8	Succinate	0.86**	- 0.83**	- 0.81**	- 0.77**
9	Glutamine	0.84**	- 0.83**	- 0.81**	- 0.95***
10	Citrate	0.65*	- 0.57	- 0.51	- 0.70*
11	Malate	0.60	- 0.51	- 0.45	- 0.57
12	Creatine	- 0.41	0.47	0.52	0.43
13	Choline	- 0.78**	0.65*	0.67*	0.77**
14	Taurine	- 0.30	0.33	0.35	0.19
15	Glucose	- 0.80**	0.79**	0.77**	0.79**
16	Glycine	- 0.41	- 0.50	- 0.61	- 0.56
17	Myo-Inositol	- 0.70*	0.69*	0.68*	0.72*
18	Lactate	0.39	- 0.28	- 0.31	- 0.43

*p<0.05, **p<0.01, ***p<0.001

Table 6.2: Tabulated summary of Pearson correlation coefficients (r) between metabolic profile of Hippocampus and the behavioural parameters.

	Metabolites	Behavioural Parameters			
		Descent Latency	Time mobile	Total distance travelled	Sucrose preference
1	Isoleucine	- 0.45	0.37	0.27	0.47
2	Leucine	- 0.41	0.27	0.18	0.41
3	Propylene Glycol	- 0.66*	0.80**	0.78	0.64*
4	3-Hydroxyisovalerate	0.45	- 0.53	- 0.42	- 0.45
5	Methylmalonate	0.47	- 0.48	- 0.38	- 0.49
6	Alanine	- 0.65*	0.51	0.40	0.62
7	Acetate	0.55	- 0.56	- 0.64*	- 0.57
8	Proline	- 0.70*	0.73*	0.71*	0.81**
9	NAA/NAAG	0.40	- 0.34*	- 0.27	- 0.46
10	Glutamate	0.53	- 0.57	- 0.59	- 0.60
11	4-Aminobutyrate	0.60	- 0.59	- 0.65*	-0.64*
12	Succinate	0.71*	- 0.80**	- 0.82**	-0.79**
13	Glutamine	0.83**	- 0.72*	- 0.67*	- 0.83**
14	Citrate	0.72*	- 0.74*	- 0.72*	- 0.75
15	Malate	0.46	0.33	0.26	0.41
16	Aspartate	0.43	- 0.40	- 0.49	- 0.32
17	Creatine	- 0.24	0.36	0.43	0.36
18	Choline	- 0.77**	0.75*	0.79**	0.89***
19	Glucose	- 0.69*	0.77**	0.79**	0.79**
20	Betaine	- 0.46	0.58	0.65*	0.62
21	Methanol	- 0.64*	- 0.67*	- 0.72*	- 0.72*
22	Taurine	- 0.40	0.48	0.51	0.53
23	Glycine	0.50	- 0.50	- 0.60	- 0.47
24	Myo-Inositol	- 0.63*	0.73*	0.75*	0.79**
25	Lactate	0.44	- 0.42	- 0.47	- 0.49
26	Tyrosine	0.83**	- 0.86**	- 0.84**	- 0.93 ***

*p<0.05, **p<0.01, ***p<0.001

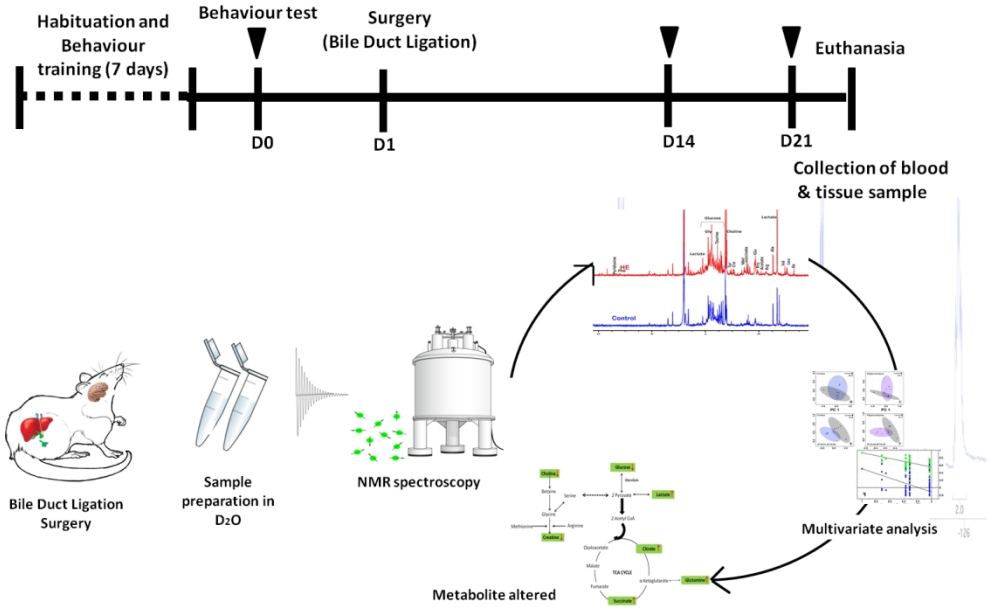

Graphical Abstract

133x95mm (300 x 300 DPI)

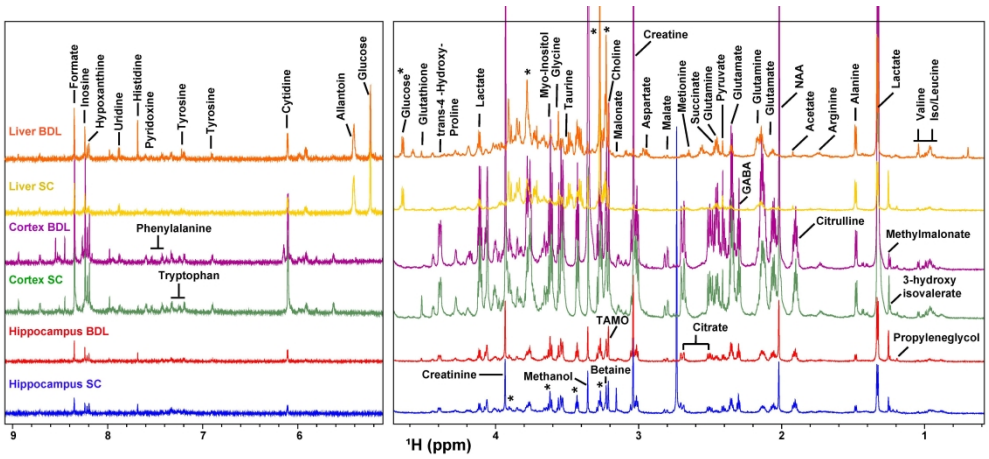

Figure 1: Stack plot of representative 1D 1H NMR spectra from liver, Cortex and hippocampus of SC and BDL animals.

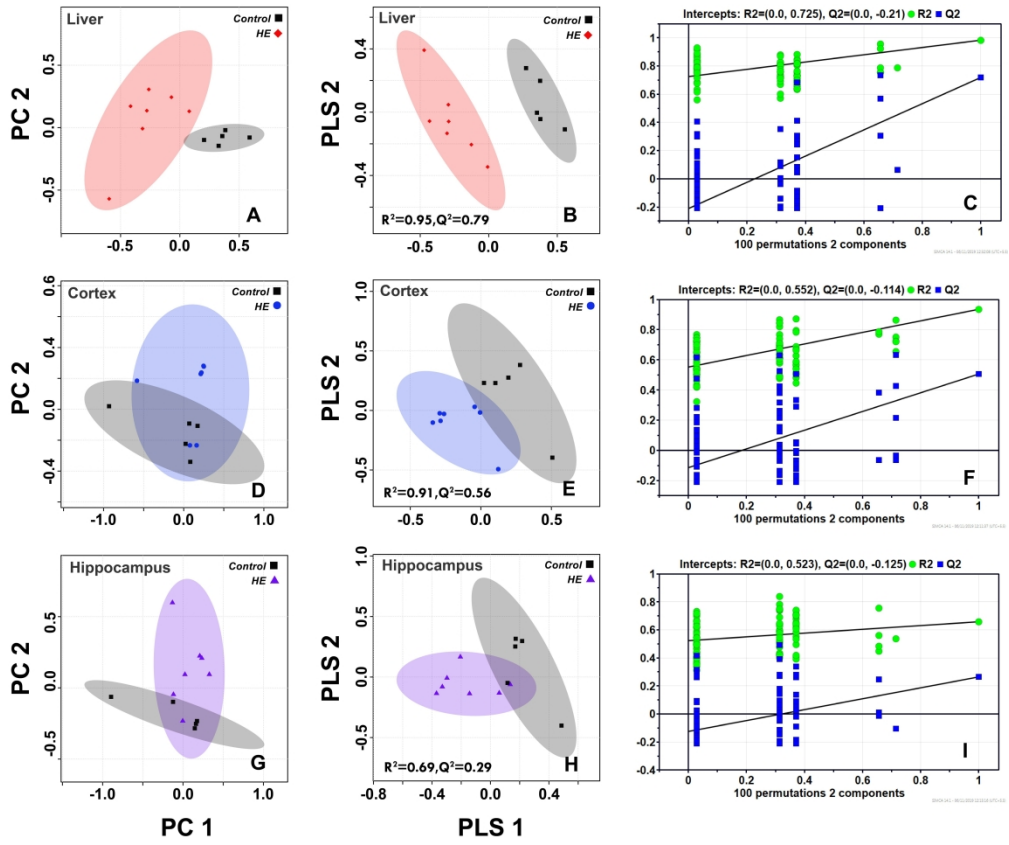

Figure 2: Two dimensional PCA and PLS-DA score plots derived from one dimensional 1H CPMG NMR spectra of liver (A, B) cortex (D, E) and hippocampus (G, H) from SC and BDL groups. Each data point denotes one subject. A 100 random permutation test for PLS-DA models generated from liver (C), cortex (F) and hippocampus (I) of control and BDL groups. The R2 value (green) represents the goodness of fit of the model. The Q2 value (blue) represents the predictability of the models.

448x377mm (300 x 300 DPI)

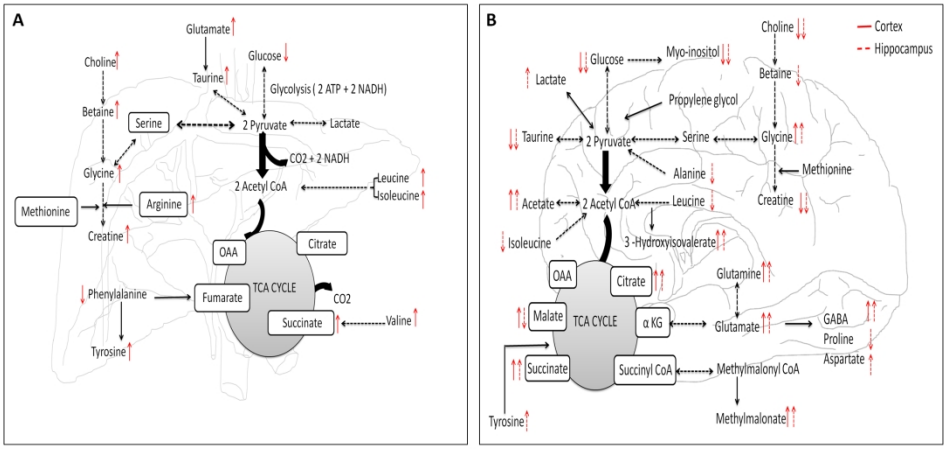

Figure 3: Metabolic pathways related to metabolites altered in the liver (A) and brain (B) of BDL animals.

216x125mm (300 x 300 DPI)

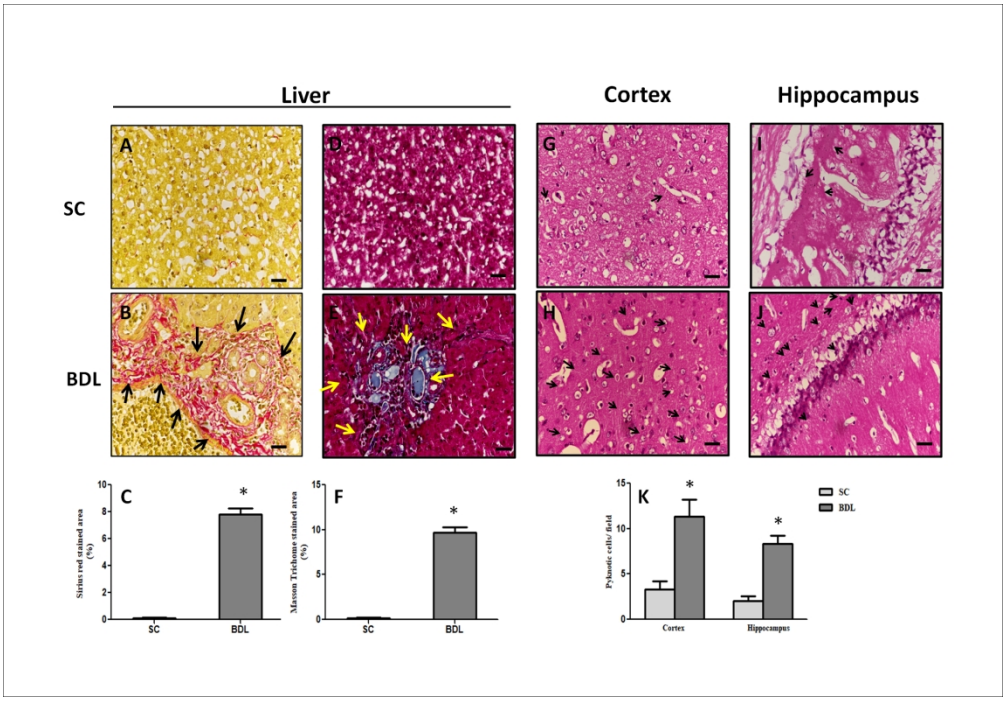

Figure 4: Photomicrographs of liver and brain sections from SC (A,D,G,I) and BDL rats (B,E,H,J) at magnification, 600X. Liver sections stained with Sirius red are shown in A and B whereas with masson trichome are reported in D and E. Arrows indicate collagen stained areas and percentage of Sirius red and masson trichome stained area analyzed using ImageJ (C and F, respectively). Cortex (G and H) and hippocampus (I and J) sections were stained with H&E. Arrows indicate pyknotic neuronal cells. Number of pyknotic cells/field analyzed using ImageJ (K). Values are expressed as mean ± SEM; n=3. *Significantly different from control group (P<0.05).

196x135mm (300 x 300 DPI)

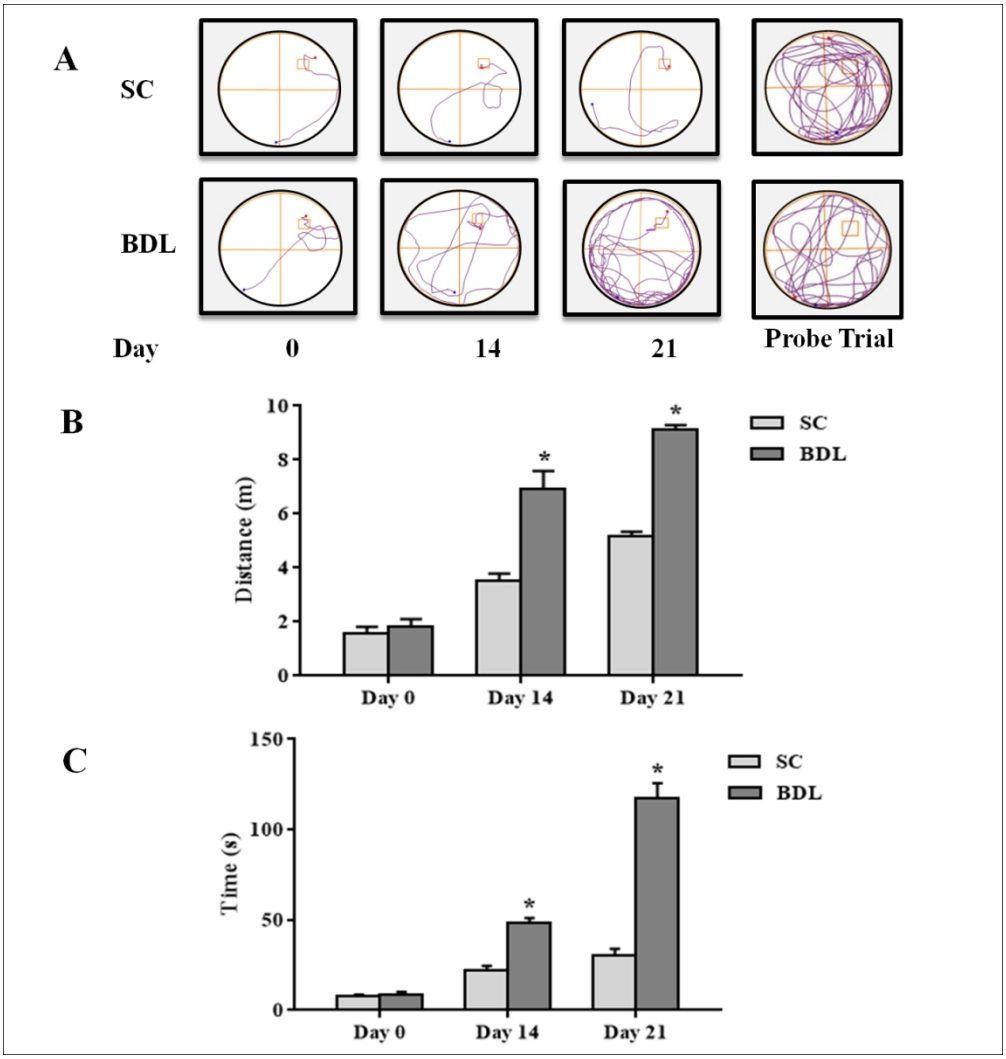

Figure 5: Effect of BDL on learning and memory assessed by Morris water maze test. Representative track plots of animals recorded using video tracking software ANY-maze (A) distance travelled (B) and total time (C). Values are expressed as mean ± SEM; n = 5. *Significantly different from SC group ($p < 0.05$).

119x125mm (300 x 300 DPI)

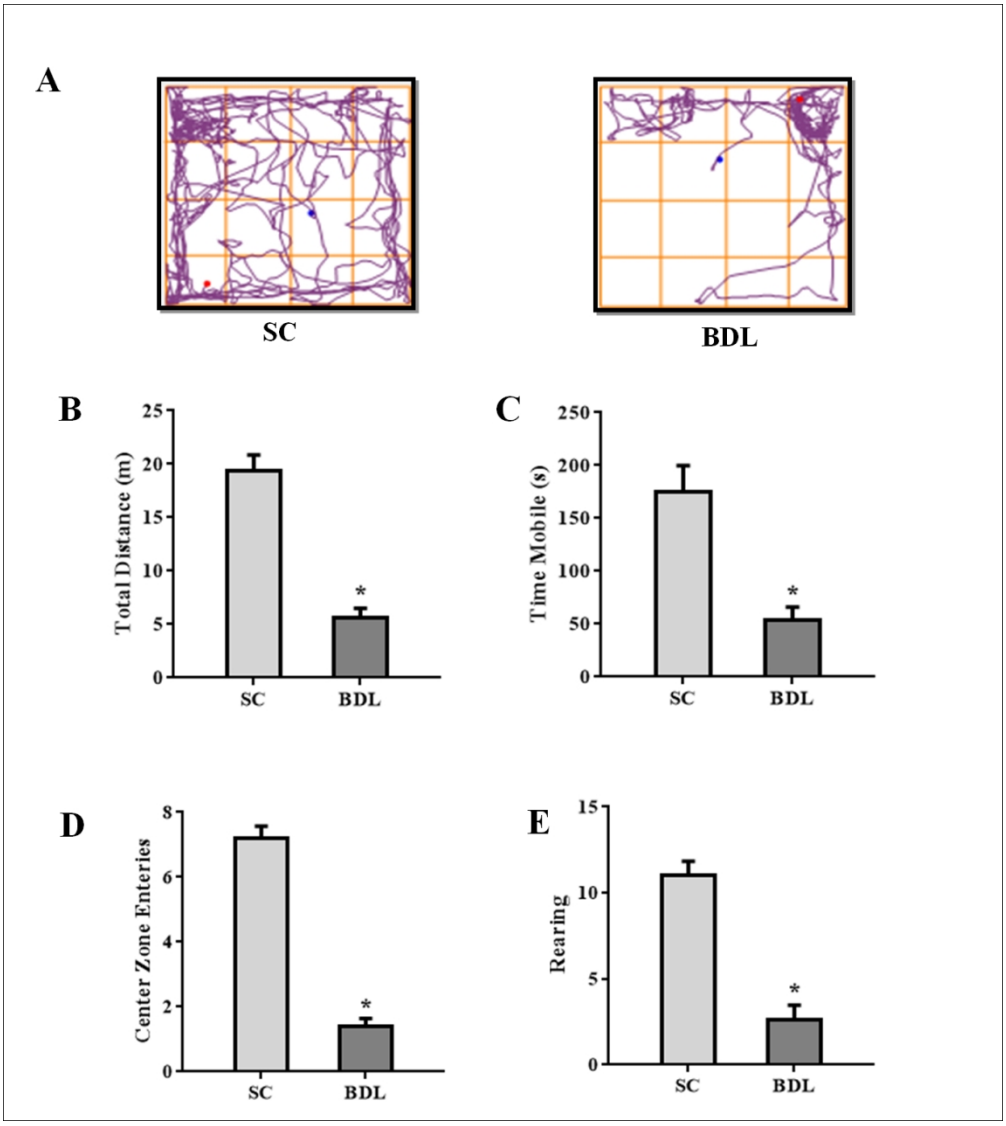

Figure 6: Effect of BDL on locomotor functions assessed by open field test. Representative track plots of animals recorded using video tracking software ANY-maze (A), total distance travelled (B) time mobile (C) No. of center zone entries (D) and Rearing frequency (E). Values are expressed as mean ± SEM; n = 5. *Significantly different from SC group ($p < 0.05$).

234x261mm (150 x 150 DPI)

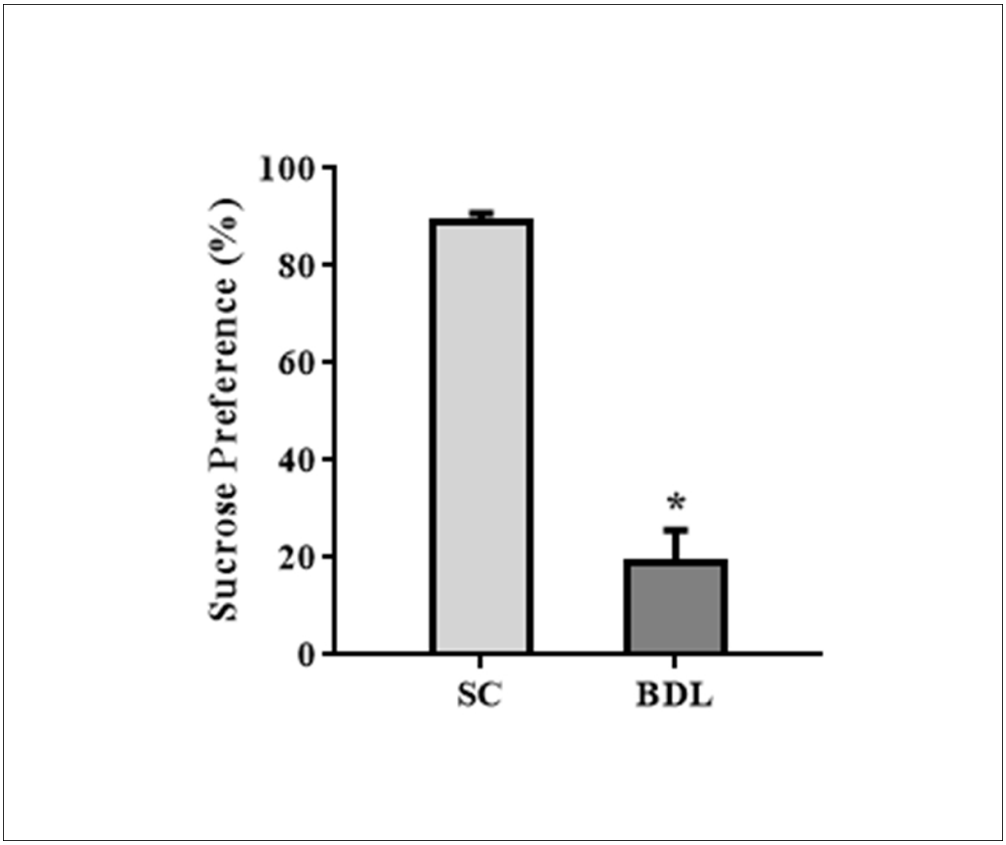

Figure 7: Effect of BDL on depressive behavior assessed by sucrose water preference test. Values are expressed as mean ± SEM; n=5. *Significantly different from SC group (P<0.005).

103x86mm (300 x 300 DPI)

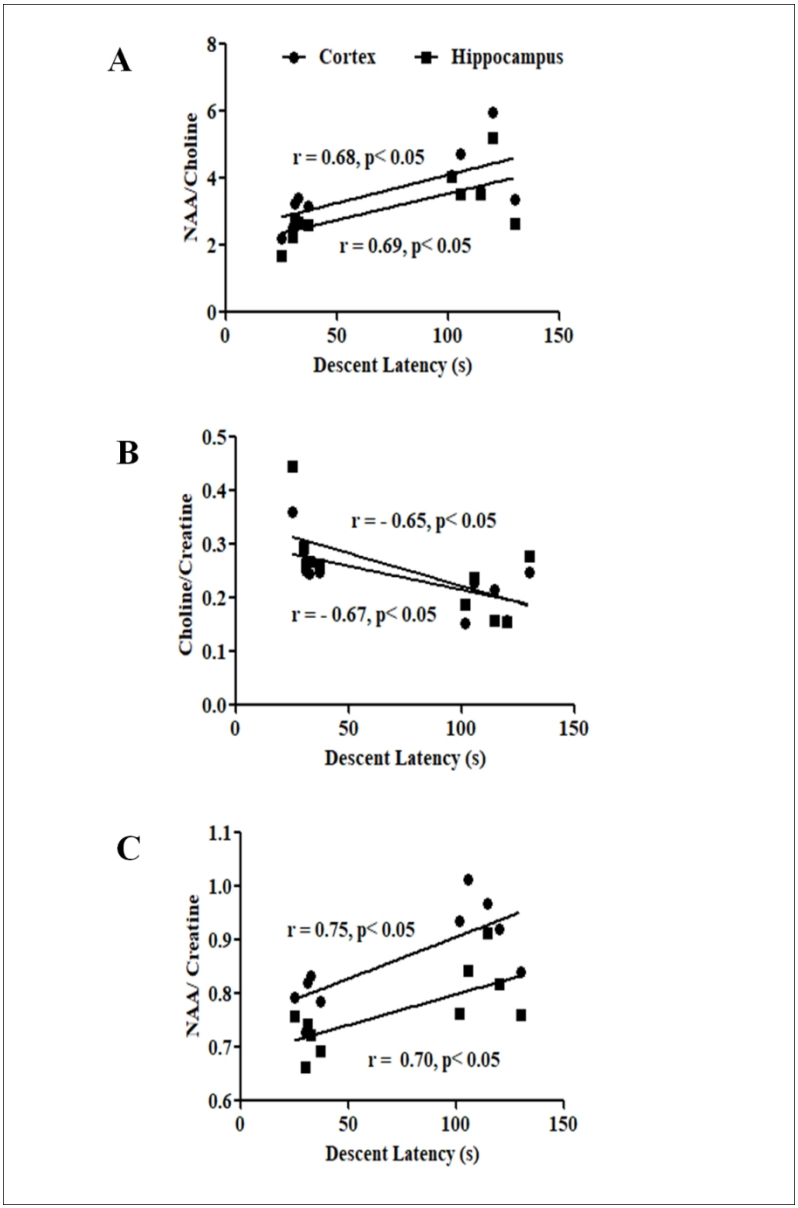

Figure 8: Correlation plots showing the relation between cognitive behaviour with the metabolic profiles from SC and BDL. Correlation between descent latency and NAA/Choline (A), Choline/Creatine (B) and NAA/Creatine (C). Two-tailed Pearson correlation were performed.

192x291mm (150 x 150 DPI)

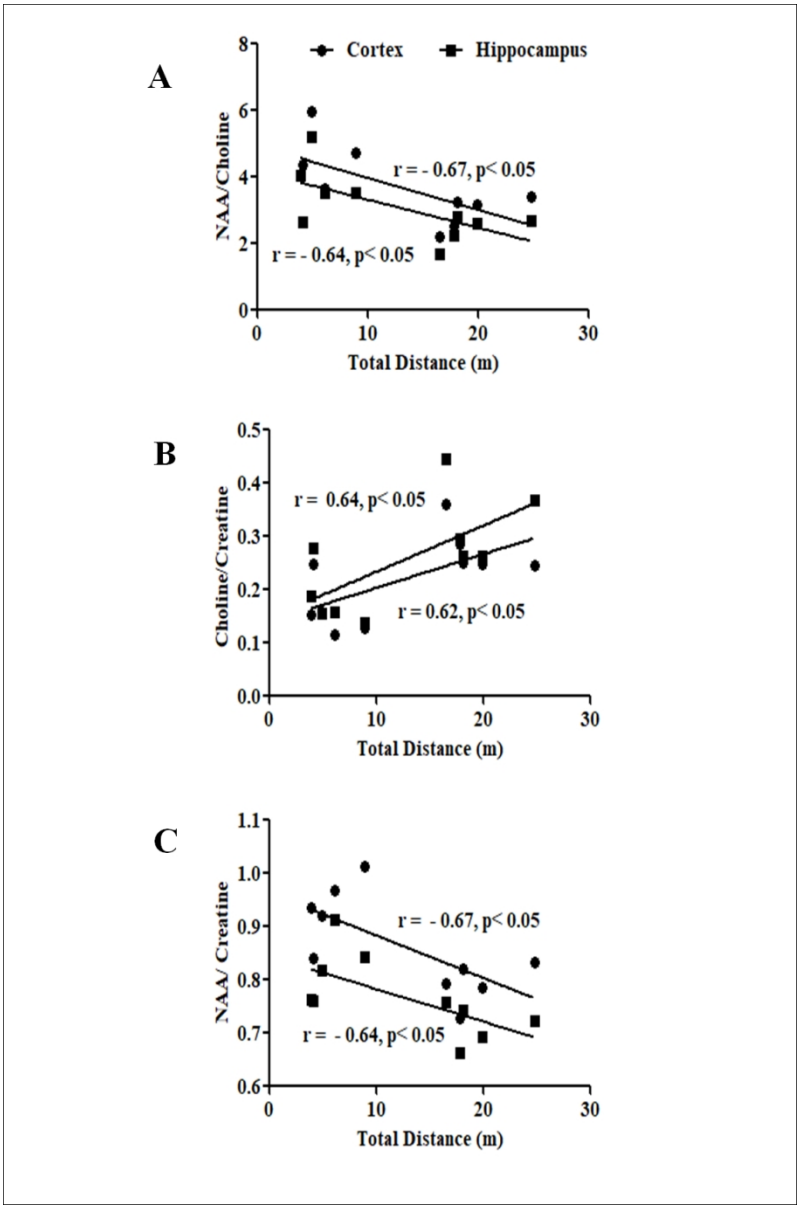

Figure 9: Correlation plots showing the relation between Motor behavior with the metabolic profiles from SC and BDL. Correlation between total distance travelled and NAA/Choline (A), Choline/Creatine (B) and NAA/Creatine (C). Two-tailed Pearson correlation were performed.

194x293mm (150 x 150 DPI)